ARTICLE

Effects of Carbide Formation in Graphene Growth

Zhun-zhun Wang, Qi-quan Luo, Wen-hua Zhang, Zhen-yu Li*

Hefei National Laboratory for Physical Sciences at the Microscale, University of Science and Technology of China, Hefei 230026, China

(Dated: Received on October 7, 2014; Accepted on October 23, 2014)

Besides carbon solubility, the carbide formation possibility is another important factor to differentiate various substrate materials in graphene growth. A recent experiment indicates that the formation of transition metal carbides (TMCs) can suppress carbon precipitation. In this study, Mo_2C, a representative of TMCs, is used to study the effects of carbide formation in graphene growth from first principles. Carbon diffusion in Mo_2C bulk turns out to be very difficult and it becomes much easier on the $Mo_2C(001)$ surface. Therefore, carbon precipitation suppression and graphene growth can be realized simultaneously. A direction depended diffusion behavior is observed on the $Mo_2C(101)$ surface, which makes it less favorable for graphene growth compared to the (001) surface.

Key words: Molybdenum carbide, Diffusion, Density functional theory

I. INTRODUCTION

Due to its unique properties and potential applications [1, 2], graphene has been intensively studied in the last decade. Among the several reported methods to synthesize graphene [3], chemical vapor deposition (CVD) is especially promising to obtain high quality samples at a large scale [4]. To optimize a CVD growth, the substrate should be carefully chosen [5]. Various metal substrates have been tried in graphene growth, and high quality monolayer graphene can be grown on some of them, such as Cu [6].

On different substrates, the graphene growth mechanisms can be very different [7−9]. To choose a suitable metal substrate, we can check metal-C phase diagrams and compare corresponding parameters including carbon solubility and carbide formation possibility [10]. Effects of the former have been intensively studied already [11]. On metal substrates with a relatively high carbon solubility, graphene growth proceeds via a precipitation mechanism, which makes a layer number control difficult to achieve [12]. In contrast, on metal substrates with negligible C solubility, such as Cu, graphene growth is limited on the surface. As a result, uniform graphene monolayer can be readily obtained [6].

The possibility of carbide formation is less studied in the context of graphene growth. Recently, Zou *et al.* [13] have successfully grown uniform monolayer graphene on early transition metals. It is suggested that the realization of a layer number control in their experiment critically depends on the carbide formation, which suppresses the upward segregation or precipitation of carbon. To fully understand the effects of carbide formation in graphene growth, it is desirable to study the atomic details of relevant processes such as carbon diffusion in carbide.

In this study, using Mo as an example, effects of carbide formation in graphene growth are studied from first principles. According to Mo-C phase diagram [14], the stable carbide phase at a typical growth temperature (1050 °C) is Mo_2C. Carbon diffusion in Mo_2C bulk and on its surfaces is studied. Based on our calculations, a clear picture of the molybdenum carbide formation aided layer number control in graphene growth is obtained.

II. COMPUTATIONAL DETAILS

All calculations were performed with the density functional theory (DFT) implemented in the Vienna *ab initio* simulation package (VASP) [15, 16] within the projector augmented wave (PAW) framework [17], using the Perdew-Burke-Ernzerhof (PBE) exchange-correlation functional [18]. A 450 eV kinetic energy cutoff was chosen for the plane wave basis set [19]. Geometry optimizations were done until forces were smaller than 0.02 eV/Å and the energy difference was lower than 10^{-5} eV. Monkhorst-Pack k-point sampling [20] was used in our calculations with a careful convergence test. The climbing image nudged elastic band (CI-NEB) method [21] was used to locate transition states, where the residual forces were within 0.03 eV/Å. In surface calculations, slab models were constructed with vacuum zones thicker than 20 Å.

To compare the stability of different types of defects, their chemical environment should be specified, which

*Author to whom correspondence should be addressed. E-mail: zyli@ustc.edu.cn

is characterized by the chemical potentials of Mo and C. Considering the equilibrium with Mo_2C bulk, we have

$$E^{\rm bulk}_{\rm Mo_2C} = 2\mu_{\rm Mo} + \mu_{\rm C} \quad (1)$$

which leaves us a single parameter ($\mu_{\rm C}$ is selected in this study). In C-rich conditions, $\mu_{\rm C}$ approaches the energy of a free carbon atom which is set to zero. In C-poor conditions, we set the boundary of $\mu_{\rm C}$ as $E^{\rm bulk}_{\rm Mo_2C} - 2E^{\rm bulk}_{\rm Mo}$, which leads to a C chemical potential range from -7.096 eV to 0 eV. Then, the formation energy of a C vacancy or a doped/adsorbed carbon can be defined as

$$E_{\rm form} = E_{\rm tot} - E_{\rm pristine} \pm \mu_{\rm C} \quad (2)$$

where $E_{\rm tot}$ is the energy of the whole system and $E_{\rm pristine}$ is the energy of Mo_2C bulk or surface without defect. The positive and negative signs correspond to carbon vacancy and doped/adsorbed carbon, respectively.

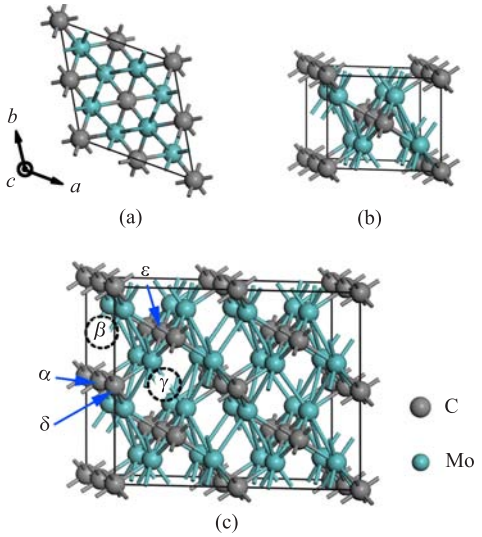

FIG. 1 (a) Top view and (b) side view of Mo_2C unit cell. (c) A 2×1×2 supercell with some atomic sites marked.

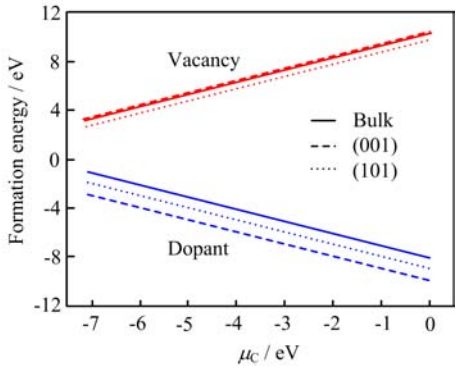

FIG. 2 Formation energy of carbon adatom/dopant and vacancy in Mo_2C bulk and surface systems.

III. RESULTS AND DISCUSSION

A. Carbon diffusion in Mo_2C bulk

There are mainly two Mo_2C crystalline structures, *i.e.* the orthorhombic [22] and hexagonal [23, 24] phases. Following previous studies [25, 26], we focus on the hexagonal phase, where Mo atoms form a hexagonally close packed structure and carbon atoms fill half of the octahedral interstitial sites (Fig.1). Each interstitial site has six neighboring Mo atom. There are two types of C and Mo atoms, forming different layers perpendicular to the c axis. The calculated lattice parameters are a=2×3.04 Å, b=2×3.04 Å, and c=4.72 Å, in good agreement with experiment values [27]. Distance between two octahedral sites in the ab plane is 2.63 Å, and along the c direction it is 2.36 Å.

Since only half of the octahedral interstitial sites are occupied by C, a natural C diffusion pathway in Mo_2C bulk is from an occupied to a neighboring unoccupied octahedral site. C diffusion can also proceed via defects, such as C vacancy and C interstitial, in Mo_2C bulk. Before discussing these diffusion pathways, we first check the thermodynamic stabilities of different types of defects. Since it brings no obvious structure deformation, a 2×1×2 supercell is used to study carbon vacancy. However, if an extra C atom is doped in the Mo_2C bulk, a structure relaxation around the dopant atom is found. Therefore, a larger 2×2×2 supercell is built to ensure that any two neighboring doping carbon atoms are separated more than 12 Å away and thus basically interaction free. As shown in Fig.2, in the whole range of $\mu_{\rm C}$, formation energy of C vacancy is positive while that of interstitial C dopant is negative. Therefore, C vacancy is thermodynamically unfavorable even in C-poor conditions (low C chemical potential), while C atom doping can be easily realized especially in C-rich conditions (high C chemical potential).

For intrinsic C diffusion from an occupied C site to a neighboring unoccupied octahedral site, there are two possible diffusion directions according to the hexagonal symmetry. We name the occupied C site as site α, the neighboring octahedral site along the c axis as site β and that within the ab plane as site γ (Fig.1(c)). In pristine bulk phase, these two unoccupied sites are equivalent. However, if α site carbon is removed, symmetry between sites β and γ is broken in our model. From site α to site β, the diffusion barrier is 2.65 eV and the final state is 1.17 eV higher in energy than the initial state. From site α to site γ, the diffusion barrier is 3.56 eV and the final state becomes 2.00 eV higher in energy.

For a C dopant at site β, diffusion to a neighboring octahedral site within the ab plane has an energy barrier of 2.59 eV. The initial and final states are equivalent. From site β, a C dopant can also diffuse to a farther octahedral site (site γ in Fig.1(c)). However, there is

DOI:10.1063/1674-0068/28/cjcp1410170

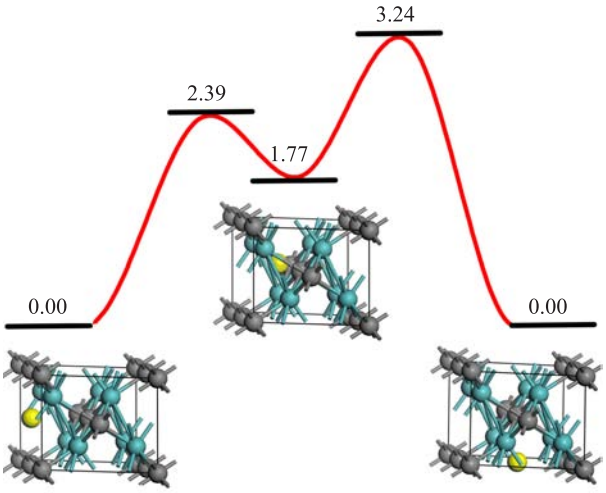

FIG. 3 The diffusion pathway of a C dopant (highlighted in yellow) in Mo_2C bulk from site β to site γ. Energy is given in eV. Geometries of the initial, intermediate, and final states are illustrated in a 1×1×1 unit cell.

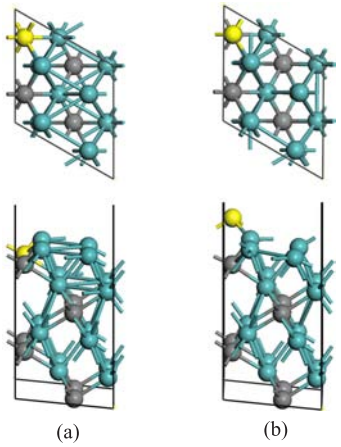

FIG. 4 (a) The $Mo_2C(001)$ surface and (b) the corresponding structure with a surface C atom lifted up as an adatom. This atom is highlighted in yellow. For both structures, top view is shown in the upper panel and side view is shown in the down panel.

an intermediate state in the diffusion path, as shown in Fig.3. The intermediate state is 1.77 eV higher in energy, where the C dopant is located at a tetrahedral site. To diffuse from β to γ, two successive energy barriers of 2.39 and 1.47 eV should be conquered.

Although it is thermodynamically not very favorable, we have also studied vacancy mediated diffusion for completeness. Considering a C atom at site α, there are two kinds of neighboring vacancy sites which can help C diffusion: sites δ and ε as shown in Fig.1(c). The $\alpha\delta$ and $\alpha\varepsilon$ distances are 3.03 and 3.84 Å, respectively. If there is a C vacancy at site δ, carbon diffusion from α to δ needs to conquer a barrier of 3.81 eV. The diffusion barrier for the α to ε path is 2.77 eV. There is no energy difference between the initial and final states in vacancy mediated C diffusion.

Therefore, carbon diffusion in Mo_2C bulk is always associated with a very high energy barrier, which will thus be difficult even at a graphene growth temperature (typically about 1300 K). As a result, the formation of molybdenum carbide can effectively suppress carbon segregation/precipitation, as indicated in the experiment [13]. Notice that the consistency among different diffusion pathways observed in this work suggests that a similar conclusion will be obtained even for a more realistic structure model of Mo_2C with C randomly occupying half of the octahedral sites [23, 24].

B. Carbon diffusion on Mo_2C surfaces

Since graphene is always grown on a surface, it is thus very desirable to study carbon diffusion on Mo_2C surfaces as well. According to previous studies [19, 25−30], the (101) surface is the most stable one. At the same time, the high-symmetry (001) surface is expected to be relevant in graphene growth [13]. Therefore, both surfaces are considered in this study. To facilitate graphene growth, an Mo-terminated model is adopted for the $Mo_2C(001)$ surface. In order to study carbon diffusion on these two surfaces, a 2 unit-cell slab for the (001) surface and a 1/4 unit-cell slab for the (101) surface are built. Within the surface plane, a 1×1 unit cell is large enough since the lattice parameters are larger than 6 Å.

Similar to the bulk case, we first study the stability of C vacancy and adsorbed C atom on the surfaces. C vacancy on the (001) surface is below the topmost Mo atom layer. The (101) surface has a notable structure relaxation compared to the bulk structure, where the outmost Mo atoms shrink towards bulk by ∼0.40 Å and other surface atoms move upward by ∼0.10 Å. Such a structure relaxation smoothes the surface. If a carbon atom on the (101) surface is removed, there is no obvious further structure relaxation. As shown in Fig.2, the formation energies of C vacancy on both Mo_2C (001) and (101) surfaces are positive, suggesting that forming C vacancy on these surfaces is also thermodynamically unfavorable as in the bulk case. Vacancies on the (001) surface and in the bulk have similar formation energy, which may be due to the fact that carbon locations on the (001) surface are closer to their bulk locations compared to the (101) surface.

Carbon adatom on these two surfaces has a negative formation energy, which is thermodynamically even more favorable than interstitial C doping in the bulk. Due to its Mo-terminated character, carbon adsorption on the (001) surface is 1.02 eV more favorable than on the (101) surface. C adsorption on Mo_2C surfaces is more stable than C doping in the bulk.

The first C diffusion process we considered is lifting up a surface atom to get an adatom, which creates a thermodynamically unfavorable C vacancy and a favor-

DOI:10.1063/1674-0068/28/cjcp1410170

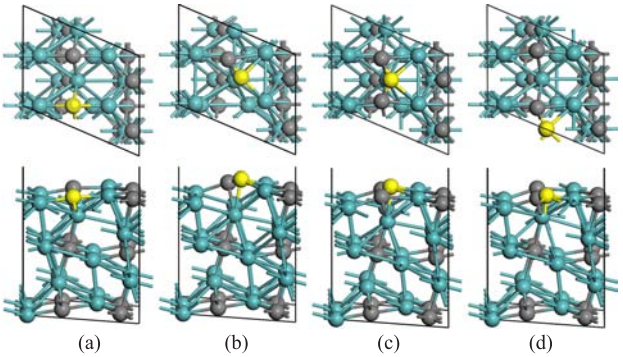

FIG. 5 (a) The $Mo_2C(101)$ surface and (b) the corresponding structure with a surface C atom lifted up as an adatom. This atom is highlighted in yellow. (c) The most stable structure of a C adatom on the (101) surface and (d) the structure with the C adatom moved to a neighboring adsorption site in the [010] direction. For all structures, top view is shown in the upper panel and side view is shown in the down panel.

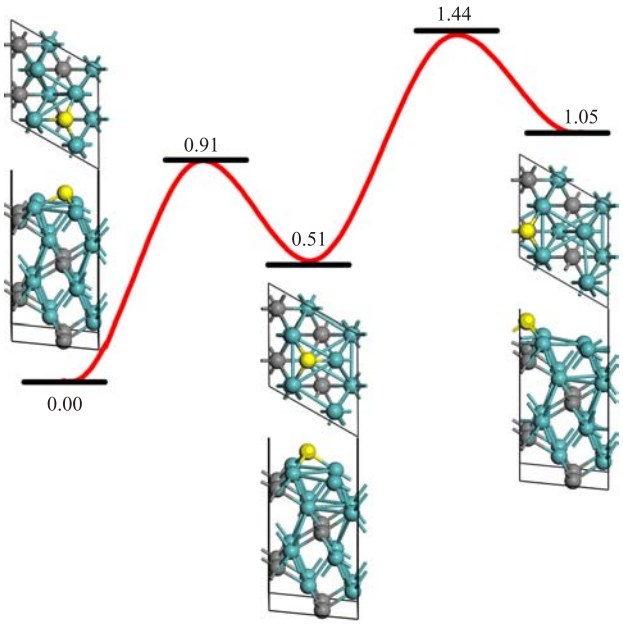

FIG. 6 Diffusion of C adatom (highlighted in yellow) on the (001) surface from O-site to T-site and then C-site. Relative energies compared to the most stable adsorption structure are given in eV.

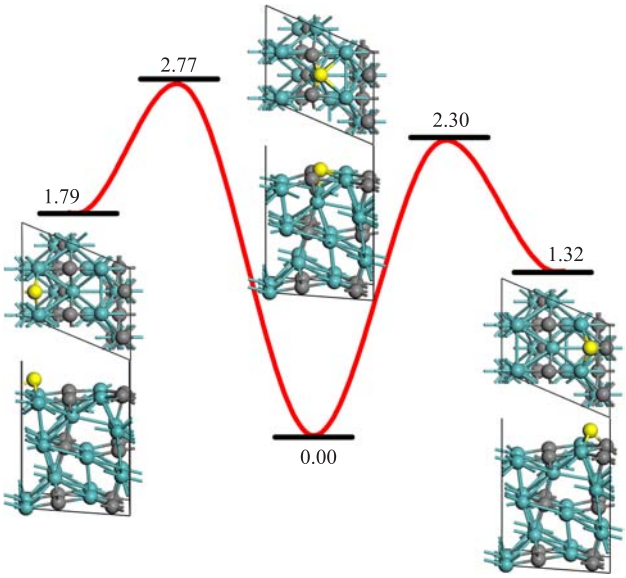

FIG. 7 Diffusion of C adatom (highlighted in yellow) on the (101) surface in the [100] direction. Relative energies compared to the most stable adsorption structure are given in eV.

able C adatom simultaneously. On the $Mo_2C(001)$ surface, such a diffusion process (in Fig.4 from (a) to (b)) has a 0.42 eV energy increase. The diffusion barrier is 1.33 eV, which is only about half of the value in the bulk case due to the structure flexibility on the surface. On the $Mo_2C(101)$ surface, the first surface layer contains both Mo and C atoms. If a carbon atom in the first surface layer is pulled up (in Fig.5 from (a) to (b)), there is a 1.80 eV diffusion barrier. The C adatom has a very different chemical environment compared to bulk C, and the final state is 0.44 eV higher in energy than the initial state. On both surfaces, vertical C diffusion is easier than C diffusion in the bulk.

Another important surface process also relevant to graphene growth is lateral C diffusion on the surface. On the $Mo_2C(001)$ surface, the most stable adsorption site is a hollow site above an octahedral interstitial site (O-site) as shown in Fig.6. The neighboring metastable site is a hollow site above a tetrahedral interstitial site (T-site). From O-site to T-site, the diffusion barrier is 0.91 eV and the reversed barrier is 0.40 eV. The next adsorption state is a hollow site above a C atom (C-site), which is 1.05 eV higher in energy than the O-site. The diffusion barrier from T-site to C-site is 0.93 eV and the reversed barrier is 0.39 eV. In general, C diffusion on (001) surface is much easier than in the bulk.

There are more metastable adsorption sites on the $Mo_2C(101)$ surface due to its lower symmetry compared to the (001) surface. The most stable adsorption structure is shown in Fig.5(c). Diffusion along the [010] direction to a neighboring stable structure (Fig.5(d)) has an energy barrier of 1.19 eV. Diffusion from the most stable adsorption site in the [100] direction has two final states (Fig.7), which are 1.79 and 1.32 eV higher in energy. The diffusion barrier in this direction is at least 2.30 eV, much higher than that in the [010] direction. Therefore, diffusion on the (101) surface is anisotropic, different from the (001) surface.

IV. CONCLUSION

According to our calculations, carbon diffusion in Mo_2C is very difficult. Although the energy barrier

DOI:10.1063/1674-0068/28/cjcp1410170

for surface vacancy formation is relatively low, Mo_2C surfaces are still not able to act as a sink or source for bulk vacancies, since vacancy mediated C diffusion in the bulk is too difficult. The same conclusion can be applied to interstitial C dopant atoms. As a result, kinetically both C vacancy and C dopant will not be massively formed in the bulk, consisting with the high thermal stability of molybdenum carbide. Notice that the formation of C vacancy is also thermodynamically unfavorable. In the context of graphene growth, Mo_2C can effectively block carbon segregation/precipitation.

Carbon diffusion on $Mo_2C(001)$ surfaces typically associates an energy barrier $\sim$1 eV, which is not prohibitive at the high temperature during graphene growth. This result is consistent with the experimental observation that high quality graphene can be grown on the Mo substrate, where carbide is formed during graphene growth. On the (101) surface, C diffusion is anisotropic, with the highest diffusion barrier as high as 2.77 eV, which is not favorable for graphene growth. In this work, only Mo_2C is studied. However, since all carbide-forming groups IVB-VIB metals show similar behaviors in the graphene growth experiment, similar conclusions are expected to be obtained for other carbides.

V. ACKNOWLEDGMENTS

This work was supported by the Ministry of Science and Technology of China (No.2014CB932700), the National Natural Science Foundation of China (No.21173202, No.21103156, and No.21222304), and the Fundamental Research Funds for the Central Universities.

[1] A. H. Castro Neto, F. Guinea, N. M. R. Peres, K. S. Novoselov, and A. K. Geim, Rev. Mod. Phys. **81**, 109 (2009).
[2] K. S. Novoselov, V. I. Falko, L. Colombo, P. R. Gellert, M. G. Schwab, and K. Kim, Nature **490**, 192 (2012).
[3] F. Bonaccorso, A. Lombardo, T. Hasan, Z. Sun, L. Colombo, and A. C. Ferrari, Mater. Today **15**, 564 (2012).
[4] S. Bae, H. Kim, Y. Lee, X. Xu, J. S. Park, Y. Zheng, J. Balakrishnan, T. Lei, H. R. Kim, and Y. I. Song, Nat. Nanotechnol. **5**, 574 (2010).
[5] N. C. Bartelt and K. F. McCarty, MRS Bull. **37**, 1158 (2012).
[6] X. S. Li, W. W. Cai, J. H. An, S. Y. Kim, J. H. Nah, D. X. Yang, R. Piner, A. Velamakanni, I. H. Jung, E. Tutuc, S. K. Banerjee, L. Colombo, and R. S. Ruoff, Science **324**, 1312 (2009).
[7] P. Wu, W. H. Zhang, Z. Y. Li, and J. L. Yang, Small **10**, 2136 (2014).
[8] P. Wu, H. J. Jiang, W. H. Zhang, Z. Y. Li, Z. H. Hou, and J. L. Yang, J. Am. Chem. Soc. **134**, 6045 (2012).
[9] W. H. Zhang, P. Wu, Z. Y. Li, and J. L. Yang, J. Phys. Chem. C **115**, 22360 (2011).
[10] C. P. Deck and K. Vecchio, Carbon **44**, 267 (2006).
[11] X. Li, W. Cai, L. Colombo, and R. S. Ruoff, Nano Lett. **9**, 4268 (2009).
[12] L. Fu, C. H. Zhang, Y. F. Zhang, and Z. F. Liu, Acta Chim. Sin. **71**, 308 (2013).
[13] Z. Y. Zou, L. Fu, X. J. Song, Y. F. Zhang, and Z. F. Liu, Nano Lett. **14**, 3832 (2014).
[14] S. Sampath and S. F. Wayne, J. Therm. Spray Technol. **3**, 282 (1994).
[15] G. Kresse and J. Furthmüller, Comp. Mater. Sci. **6**, 15 (1996).
[16] G. Kresse and J. Furthmüller, Phys. Rev. B **54**, 11169 (1996).
[17] P. E. Blöchl, Phys. Rev. B **50**, 17953 (1994).
[18] J. P. Perdew, K. Burke, and M. Ernzerhof, Phys. Rev. Lett. **77**, 3865 (1996).
[19] Q. Q. Luo, T. Wang, G. Walther, M. Beller, and H. J. Jiao, J. Power Sources **246**, 548 (2014).
[20] M. Methfessel and A. T. Paxton, Phys. Rev. B **40**, 3616 (1989).
[21] G. Henkelman, B. P. Uberuaga, and H. Jónsson, J. Chem. Phys. **113**, 9901 (2000).
[22] C. Pistonesi, A. Juan, A. P. Farkas, and F. Solymosi, Surf. Sci. **604**, 914 (2010).
[23] J. Dubois, T. Epicier, C. Esnouf, G. Fantozzi, and P. Convert, Acta Metall. **36**, 1891 (1988).
[24] T. Epicier, J. Dubois, C. Esnouf, G. Fantozzi, and P. Convert, Acta Metall. **36**, 1903 (1988).
[25] T. Wang, X. W. Liu, S. G. Wang, C. F. Huo, Y. W. Li, J. G. Wang, and H. J. Jiao, J. Phys. Chem. C **115**, 22360 (2011).
[26] J. Haines, J. Leger, C. Chateau, and J. Lowther, J. Phys.: Condens. Matter **13**, 2447 (2001).
[27] E. Rudy, S. Windisch, A. J. Stosick, and J. R. Hoffman, Trans. Metall. Soc. AIME **239**, 1247 (1967).
[28] X. R. Shi, S. G. Wang, H. Wang, C. M. Deng, Z. Qin, and J. Wang, Surf. Sci. **603**, 852 (2009).
[29] X. H. Wang, H. L. Hao, M. H. Zhang, W. Li, and K. Y. Tao, J. Solid State Chem. **179**, 538 (2006).
[30] M. Nagai, A. M. Zahidul, and K. Matsuda, Appl. Catal. A **313**, 137 (2006).

DOI:10.1063/1674-0068/28/cjcp1410170